

Anomalous electromagnetic moments of τ lepton in $\gamma\gamma \rightarrow \tau^+\tau^-$ reaction in Pb+Pb collisions at the LHC

Mateusz Dyndał,^{1,*} Mariola Klusek-Gawenda,^{2,†}
Matthias Schott,^{3,‡} and Antoni Szczurek^{§2,¶}

¹*CERN, Geneva, Switzerland*

²*Institute of Nuclear Physics Polish Academy of Sciences, PL-31342 Krakow, Poland*

³*Johannes Gutenberg University, Mainz, Germany*

(Dated: May 27, 2022)

Abstract

We discuss the sensitivity of the $\gamma\gamma \rightarrow \tau^+\tau^-$ process in ultraperipheral Pb+Pb collisions on the anomalous magnetic (a_τ) and electric (d_τ) moments of τ lepton at LHC energies. We derive the corresponding cross sections by folding the elementary cross section with the heavy-ion photon fluxes and considering semi-leptonic decays of both τ leptons in the fiducial volume of ATLAS and CMS detectors. We present predictions for total and differential cross sections, and for the ratios to $\gamma\gamma \rightarrow e^+e^-(\mu^+\mu^-)$ process. These ratios allow to cancel theoretical and experimental uncertainties when performing precision measurement of a_τ at the LHC. The expected limits on a_τ with existing Pb+Pb dataset are found to be better by a factor of two comparing to current best experimental limits and can be further improved by another factor of two at High Luminosity LHC.

PACS numbers:

arXiv:2002.05503v1 [hep-ph] 13 Feb 2020

[§] Also at Faculty of Mathematics and Natural Sciences, University of Rzeszow, ul. Pigonia 1, 35-310 Rzeszów, Poland.

*Electronic address: Mateusz.Dyndal@cern.ch

†Electronic address: Mariola.Klusek@ifj.edu.pl

‡Electronic address: mschott@cern.ch

¶Electronic address: Antoni.Szczurek@ifj.edu.pl

I. INTRODUCTION

Ultrapерipheral collisions (UPC) of heavy-ions provide a very clean environment to study various two-photon induced processes [1, 2]. Most recent examples include the production of electron pairs [3–6], muon pairs [7] and light-by-light scattering [8–10]. These reactions can also give rise to the production of tau lepton pairs, which provides a highly interesting opportunity to study the electromagnetic properties of the τ lepton via the $\text{Pb+Pb} \rightarrow \text{Pb+Pb} + \tau^+ \tau^-$ process using data from the Large Hadron Collider (LHC).

The presence of $\gamma\tau\tau$ vertex in this reaction gives sensitivity to the anomalous electromagnetic couplings of the tau lepton. Since the $\gamma\gamma \rightarrow \tau^+ \tau^-$ subprocess diagram contains two such vertices, this reaction provides even an enhanced sensitivity to the anomalous magnetic (a_τ) and electric (d_τ) moments of the τ lepton.

The strongest experimental constraints on a_τ come from the kinematics of the similar production process, $e^+e^- \rightarrow e^+e^- \tau^+ \tau^-$, measured by the DELPHI collaboration at the LEP2 collider [11] yielding a limit of

$$-0.052 < a_\tau < 0.013 \text{ (95\% CL)} . \quad (1.1)$$

The experimental limits on a_τ were also derived by the L3 and OPAL collaborations in radiative $Z \rightarrow \tau\tau\gamma$ events at LEP [12, 13], but they are typically weaker by a factor of two comparing to the DELPHI limits. For comparison, the theoretical Standard Model (SM) value of a_τ is [14, 15]:

$$a_\tau^{\text{th}} = 0.00117721 \pm 0.00000005 , \quad (1.2)$$

i.e. significantly smaller than the currently available experimental bounds.

Measuring a_τ with improved precision tests the τ lepton compositeness [16] and can be sensitive to physics beyond the Standard Model (BSM), including supersymmetric scenarios [17], left-right symmetric models [18] and unparticle physics [19].

In the $\gamma\tau\tau$ coupling, another interesting contribution is the CP-violating effects which create electric dipole moment, d_τ . The d_τ arises only at three-loop in SM and is therefore highly suppressed: $|d_\tau^{\text{th}}| < 10^{-34} e \cdot \text{cm}$ [20]; the most stringent limits on d_τ were set by Belle [21]. The presence of electric dipole moment of τ could be investigated via studying so-called CP-odd observables in $e^+e^- \rightarrow \tau^+ \tau^-$ reaction [22, 23].

There are many existing proposals how to improve the experimental sensitivity on a_τ and d_τ using lepton beams and future datasets of Belle-II [24–26], CLIC [27, 28], and LHeC [28, 29]. The LHC feasibility studies focus on the usage of proton–proton collisions [28, 30–34] and more recently also on heavy-ion UPC [35].

In this article we study the sensitivity of the $\gamma\gamma \rightarrow \tau^+ \tau^-$ process on a_τ and d_τ in Pb+Pb collisions at the LHC. We present calculations of the cross sections for the nuclear reaction, including outgoing τ decays and explicit dependence on a_τ , and considering fiducial volumes of the ATLAS [36] and CMS [37] detectors. While the authors of [35] rely on an Effective Field Theory (EFT) approach to perform predictions on the sensitivity of LHC UPC data on a_τ , we provide a first independent calculation for the $\text{Pb+Pb} \rightarrow \text{Pb+Pb} + \tau^+ \tau^-$ process for different a_τ values. We also discuss the strategy to suppress the impact of systematic uncertainties by exploiting the ratio to the $\gamma\gamma \rightarrow e^+e^- (\mu^+ \mu^-)$ processes.

II. THEORETICAL FRAMEWORK

The calculation of the process $\text{Pb}+\text{Pb}\rightarrow\text{Pb}+\text{Pb}+\tau^+\tau^-$ requires the convolution of the two-photon luminosity with the elementary $\gamma\gamma\rightarrow\tau^+\tau^-$ cross section. In our study, the nuclear cross section for the production of $\ell^+\ell^-$ pair in ultraperipheral heavy ion collision is calculated in the impact parameter space [38] and expressed via the formula:

$$\begin{aligned} \sigma(AA\rightarrow AA\ell^+\ell^-; \sqrt{s_{AA}}) &= \int \sigma(\gamma\gamma\rightarrow\ell^+\ell^-; W_{\gamma\gamma}) N(\omega_1, \mathbf{b}_1) N(\omega_2, \mathbf{b}_2) S_{abs}^2(\mathbf{b}) \\ &\times \frac{W_{\gamma\gamma}}{2} dW_{\gamma\gamma} dY_{\ell\ell} d\bar{b}_x d\bar{b}_y d^2b. \end{aligned} \quad (2.1)$$

Here b denotes the impact parameter, i.e. the distance between colliding nuclei in the plane perpendicular to their direction of motion. $W_{\gamma\gamma} = \sqrt{4\omega_1\omega_2}$ is the invariant mass of the $\gamma\gamma$ system and ω_i , $i = 1, 2$, is the energy of the photon which is emitted from the first or second nucleus, respectively. $Y_{\ell\ell}$ is the rapidity of the $\ell^+\ell^-$ system. The quantities $\bar{b}_x = (b_{1x} + b_{2x})/2$, $\bar{b}_y = (b_{1y} + b_{2y})/2$ are given in terms of b_{ix} and b_{iy} which are the components of the \mathbf{b}_1 and \mathbf{b}_2 vectors that mark the point (distance from the first and second nucleus) where photons collide and particles are produced. The diagram illustrating these quantities in the impact parameter space can be found in [38], where also the dependence of the photon flux $N(\omega_i, \mathbf{b}_i)$ on the charge form factor is presented.

Our main calculations rely on the *realistic form factor*, defined as the Fourier transform of the charge distribution in the nucleus. However, more sophisticated calculations are required for differential cross section predictions as well as for predictions in certain fiducial volumes which are typically imposed by experimental constrains. For those predictions, we introduce an additional kinematic parameter related to angular distribution for the subprocess into the underlying integration. A more detailed discussion of the nuclear cross section for the $\text{Pb}+\text{Pb}\rightarrow\text{Pb}+\text{Pb}+\ell^+\ell^-$ reaction that includes kinematic variables of outgoing leptons is given in [39].

In general, we study the $\gamma\gamma\rightarrow\ell^+\ell^-$ subprocess where the momenta of the incoming photons are denoted by p_1 and p_2 , while p_3 and p_4 denote the positively and negatively charged lepton momenta, respectively. In addition, we define $p_t = p_2 - p_4 = p_3 - p_1$ and $p_u = p_1 - p_4 = p_3 - p_2$. The amplitude for the $\gamma\gamma\rightarrow\ell^+\ell^-$ reaction in the t - and u -channel was previously derived [40] and is given by the formula:

$$\begin{aligned} \mathcal{M} &= (-i) \epsilon_{1\mu} \epsilon_{2\nu} \bar{u}(p_3) \left(i\Gamma^{(\gamma\ell\ell)\mu}(p_3, p_t) \frac{i(\not{p}_t + m_\ell)}{t - m_\ell^2 + i\epsilon} i\Gamma^{(\gamma\ell\ell)\nu}(p_{t'} - p_4) \right. \\ &\quad \left. + i\Gamma^{(\gamma\ell\ell)\nu}(p_3, p_u) \frac{i(\not{p}_u + m_\ell)}{u - m_\ell^2 + i\epsilon} i\Gamma^{(\gamma\ell\ell)\mu}(p_{u'} - p_4) \right) v(p_4). \end{aligned} \quad (2.2)$$

Here a photon-lepton vertex function is introduced that depends on the momentum transfer, $q = p' - p$. Denoting p' and p as momenta of incoming and outgoing lepton, respectively, this can be written as:

$$i\Gamma_\mu^{(\gamma\ell\ell)}(p', p) = -ie \left[\gamma_\mu F_1(q^2) + \frac{i}{2m_\ell} \sigma_{\mu\nu} q^\nu F_2(q^2) + \frac{1}{2m_\ell} \gamma^5 \sigma_{\mu\nu} q^\nu F_3(q^2) \right], \quad (2.3)$$

where $\sigma_{\mu\nu} = \frac{i}{2} [\gamma_\mu, \gamma_\nu]$ is the spin tensor that is proportional to the commutator of the gamma matrices, $F_1(q^2)$ and $F_2(q^2)$ are the Dirac and Pauli form factors, $F_3(q^2)$ is the

electric dipole form factor. The last term violates CP symmetry and its non-zero value can be evidence of physics BSM. The asymptotic values of the form factors, in the $q^2 \rightarrow 0$ limit, are the moments describing the electromagnetic properties of the lepton: $F_1(0) = 1$, $F_2(0) = a_\ell$ and $F_3(0) = d_\ell \frac{2m_\ell}{e}$. Since the virtualities of exchanged photons for ultraperipheral Pb+Pb collisions at the LHC are very small (typically $Q_{1,2}^2 < 0.001 \text{ GeV}^2$), this asymptotic condition is well fulfilled.

Finally, the differential elementary cross section for the dilepton production in the $\gamma\gamma$ -fusion reaction is given as follows:

$$\frac{d\sigma(\gamma\gamma \rightarrow \ell^+\ell^-)}{dz} = \frac{2\pi}{64\pi^2 s} \frac{|\mathbf{p}_{out}|}{|\mathbf{p}_{in}|} \frac{1}{4} \sum_{\text{spin}} |\mathcal{M}|^2, \quad (2.4)$$

where $z = \cos\theta$ and θ is an angle of the outgoing leptons relative to the beam direction in the photon-photon center-of-mass frame, s is the invariant mass squared of the $\gamma\gamma$ system, \mathbf{p}_{out} and \mathbf{p}_{in} are the 3-momenta of outgoing (lepton) and initial particle (photon), respectively.

The elementary $\gamma\gamma \rightarrow \tau^+\tau^-$ cross section strongly depends on the value of anomalous magnetic moment of τ lepton. Figure 1 illustrates the impact of non-zero a_τ value on the elementary cross section for $\gamma\gamma \rightarrow \tau^+\tau^-$ process as a function of $W_{\gamma\gamma}$ ($= m_{\tau\tau}$) and $\cos\theta$ at $W_{\gamma\gamma} = 15 \text{ GeV}$. Shown are the results for three representative values of the anomalous magnetic moment, $a_\tau = +0.1$ (green dotted line), $a_\tau = 0$ (red solid line) and $a_\tau = -0.1$ (black dashed line), respectively.

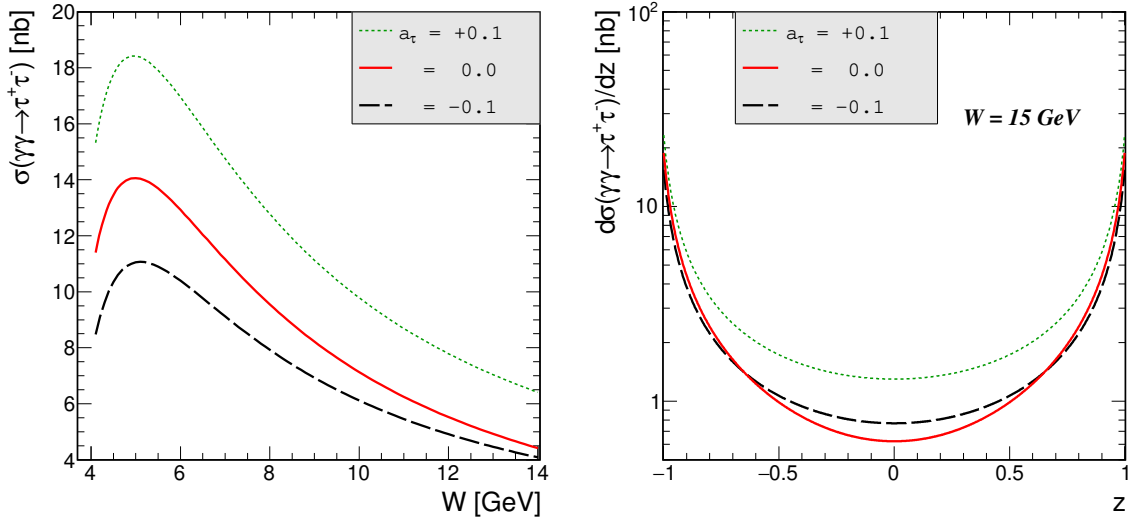


FIG. 1: Elementary cross section for $\gamma\gamma \rightarrow \tau^+\tau^-$ process as a function of $W_{\gamma\gamma} = m_{\tau\tau}$ (left) and as a function of $z = \cos\theta$ for $W_{\gamma\gamma} = 15 \text{ GeV}$ (right).

Fig. 2 shows the ratio of the total (integrated) nuclear cross section for τ pair production in Pb+Pb collisions at $\sqrt{s_{NN}} = 5.02 \text{ TeV}$ with respect to the results with $a_\tau = 0$ (SM). We show the results both for the full momentum space (black solid line) and with extra requirement of $p_T^\tau > 1 \text{ GeV}$ (blue dashed line). The total cross section values for $a_\tau = 0$ are: $\sigma(\text{Pb+Pb} \rightarrow \text{Pb+Pb}+\tau^+\tau^-; p_T^\tau > 0 \text{ GeV}) = 1.06 \text{ mb}$ and $\sigma(\text{Pb+Pb} \rightarrow \text{Pb+Pb}+$

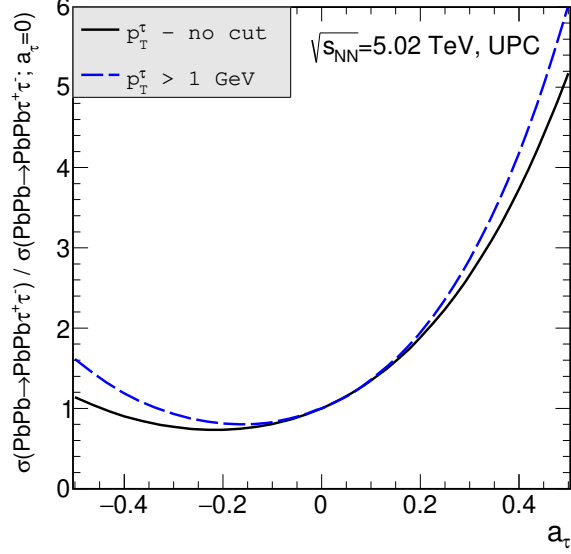


FIG. 2: Ratio of the total nuclear cross sections for $\text{Pb}+\text{Pb}\rightarrow\text{Pb}+\text{Pb}+\tau^+\tau^-$ production at the LHC energies as a function of a_τ , relative to SM ($a_\tau = 0$). The ratio of the cross sections with extra $p_T^\tau > 1$ GeV requirement applied is also shown.

$\tau^+\tau^-; p_T^\tau > 1$ GeV) = 0.73 mb. The relative cross section changes significantly with a_τ , while its dependence on the p_T^τ cut value is relatively small for $|a_\tau| < 0.1$.

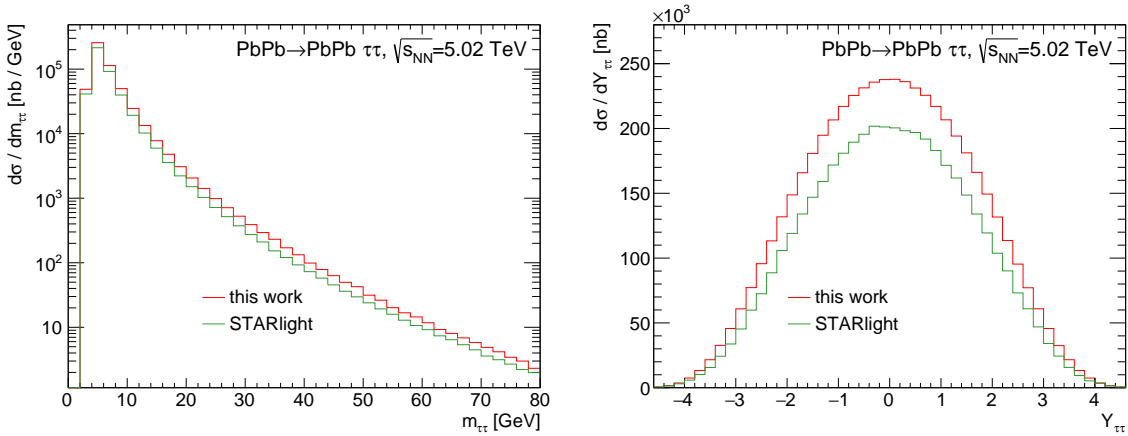


FIG. 3: Total cross section for $\text{Pb}+\text{Pb}\rightarrow\text{Pb}+\text{Pb}+\tau^+\tau^-$ production at the LHC energies as a function of ditau invariant mass (left) and ditau rapidity (right). Our results are compared with the results obtained from the STARLIGHT MC generator.

We also compare our results ($a_\tau = 0$) with STARLIGHT Monte Carlo generator [41], which is commonly used to describe ultraperipheral heavy-ion collision data. Figure 3 shows the comparison of total cross section for $\text{Pb}+\text{Pb}\rightarrow\text{Pb}+\text{Pb}+\tau^+\tau^-$ production as a function of $m_{\tau\tau}$ and $Y_{\tau\tau}$. In general, the predictions from STARLIGHT are systematically lower by about 20% in comparison to the results of the calculations described above. The overall shape of the $m_{\tau\tau}$ distribution is also slightly different between the two cal-

culations. This is mainly because STARLIGHT applies extra $|\mathbf{b}_1| > R_{pb}$ and $|\mathbf{b}_2| > R_{pb}$ requirements in the modelling of photon fluxes (see Eq. (2.1)). However, as it will be shown in Sec. IV, the modeling uncertainty of incoming photon fluxes cancel out to a large extent, once the ratio of various $\gamma\gamma \rightarrow \ell^+\ell^-$ ($\ell = e, \mu, \tau$) cross sections is used.

III. FIDUCIAL SELECTION AND τ DECAYS

In order to study the experimental sensitivity on a_τ in the $\gamma\gamma \rightarrow \tau^+\tau^-$ processes at the LHC, one has to record UPC events, which contain two reconstructed tau candidates and no further activity in the detector. Since the tau is the heaviest lepton with a lifetime of 3×10^{-13} s, it decays into lighter leptons (electron or muon) or hadrons (mainly pions and kaons) before any direct interaction with the detector material. The reconstruction of tau candidates depends therefore on the identification of its unique decay signatures. The primary τ decay channels produce one charged particle in the final state, denoted as $1ch$, or one-prong decays in the following,

$$\tau^\pm \rightarrow \nu_\tau + \ell^\pm + \nu_\ell \quad (\ell = e, \mu), \quad (3.1)$$

$$\tau^\pm \rightarrow \nu_\tau + \pi^\pm + n\pi^0, \quad (3.2)$$

or three charged particles, denoted as $3ch$, or three-prong decays, i.e.

$$\tau^\pm \rightarrow \nu_\tau + \pi^\pm + \pi^\mp + \pi^\pm + n\pi^0. \quad (3.3)$$

Approximately 80% of all τ decays are the one-prong decays and 20% of them are the three-prong decays.

While the differential cross sections of $\text{Pb+Pb} \rightarrow \text{Pb+Pb} + \tau^+\tau^-$ at the LHC are based on the previous calculations, the PYTHIA8.243 program [42] is used to model τ decays for our studies, as it simulates all known τ decay channels with a branching fraction greater than 0.04%, including large number of 2- to 6-body decay modes [43]. The effect of QED final state radiation (FSR) from outgoing leptons is also simulated by PYTHIA8. However, the spin correlations for τ decays are not taken into account, as this feature is currently not supported for the $\gamma\gamma \rightarrow \tau^+\tau^-$ process within PYTHIA8.

We propose that the $\gamma\gamma \rightarrow \tau^+\tau^-$ candidates events are selected by requiring at least one τ lepton to decay leptonically, as this allows that existing triggering algorithms of the ATLAS or CMS detector can be used [36, 37]. The leading electron or muon is further required to have a transverse momentum of $p_T > 4$ GeV and $|\eta| < 2.5$ to allow for an efficient reconstruction and identification by the LHC detectors. The correlation between the p_T of one tau and its charged decay lepton is shown in Figure 4, indicating a broad smearing of the decay lepton p_T due to the presence of neutrinos. On the contrary, there is a good correlation between the rapidity of $\tau^+\tau^-$ system and the rapidity of the final-state charged-particle system, as shown in Fig. 4 (right).

It should be noted that the majority of produced τ lepton pairs have relatively low energy/transverse momentum. Therefore, the standard τ identification tools, developed by the ATLAS and CMS collaborations [44, 45] are not expected to be applicable. We propose therefore to categorize the $\gamma\gamma \rightarrow \tau^+\tau^-$ candidate events by their decay mode:

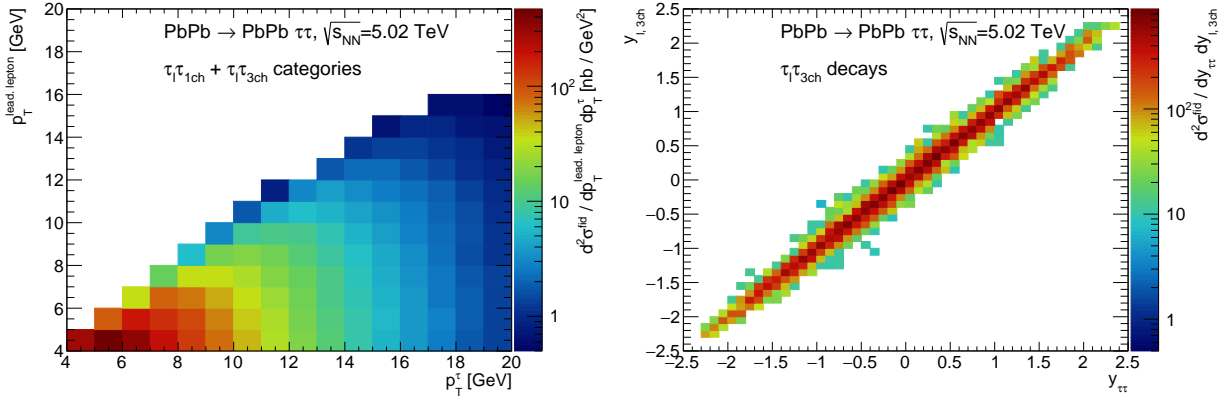


FIG. 4: (left) Correlation between p_T of the τ lepton and p_T of the electron (muon) from its decay for both event categories. (right) Correlation between the rapidity of $\tau^+\tau^-$ system and the rapidity of the final-state charged-particle system for $\tau_\ell\tau_{3ch}$ category. The results are obtained for SM scenario ($a_\tau = 0$) with full set of fiducial cuts applied.

$\tau_\ell\tau_{1ch}$ ¹ or $\tau_\ell\tau_{3ch}$. All charged-particle tracks from τ_{1ch} or τ_{3ch} decays are required to have a transverse momentum of $p_T > 0.2$ GeV and a pseudo-rapidity of $|\eta| < 2.5$.

Possible background processes which could fake the $\gamma\gamma \rightarrow \tau^+\tau^-$ signal are: the two-photon quark-antiquark production ($\gamma\gamma \rightarrow q\bar{q}$) and the (semi)exclusive production of electron/muon pairs. As demonstrated already in Ref. [35], the $\gamma\gamma \rightarrow q\bar{q}$ have a significantly larger charged-particle multiplicity than the signal and hence this background is fully reducible by exclusivity requirements.

On the other hand, the $\gamma\gamma \rightarrow \ell^+\ell^-$ production can become an irreducible background for the $\tau_\ell\tau_{1ch}$ category. To suppress this background, additional requirements on p_T of the lepton+track system ($p_T^{\ell\ ch} > 1$ GeV) have to be applied for this event category. As presented in Figure 5, an increased $p_T^{\ell\ ch} > 1$ GeV cut removes only 10% of signal events, however, suppresses at the same time significantly back-to-back $\gamma\gamma \rightarrow e^+e^-$ ($\mu^+\mu^-$) processes and leading therefore to negligible background contribution from this process.

A further possible source of background is the semi-coherent dilepton production, i.e. $\gamma^*\gamma \rightarrow \ell^+\ell^-$. Here, the p_T of the dilepton system can be as large as $p_T^{\ell\ ch}$ in the signal process. Due to relatively large momentum transfer from γ^* , the outgoing ion dissociates, emitting forward neutrons detectable in ZDC systems [46]. Thus a requirement of zero neutrons in both ion directions provides a straightforward way to estimate and even fully suppress this background. Since the neutrons can be occasionally emitted also in the signal process due to extra Coulomb exchanges [47], a full neutron veto can lead to 20–30% reduction of the cross sections. The study of the neutron emissions is, however, beyond the scope of this paper.

The differential fiducial cross section as a function of leading lepton p_T for all event categories is also shown in Figure 5. The majority of selected events have a single charged pion in the final state due to the relatively large branching fraction. These events are followed by fully leptonic decays of both τ leptons. The $\tau_\ell\tau_{1ch}$ category has the lowest cross

¹ due to the presence of soft lepton tracks, experimentally these leptons cannot be easily distinguished from pions, hence fully leptonic decays of both τ are kept as a part of a more generic $\tau_\ell\tau_{1ch}$ category

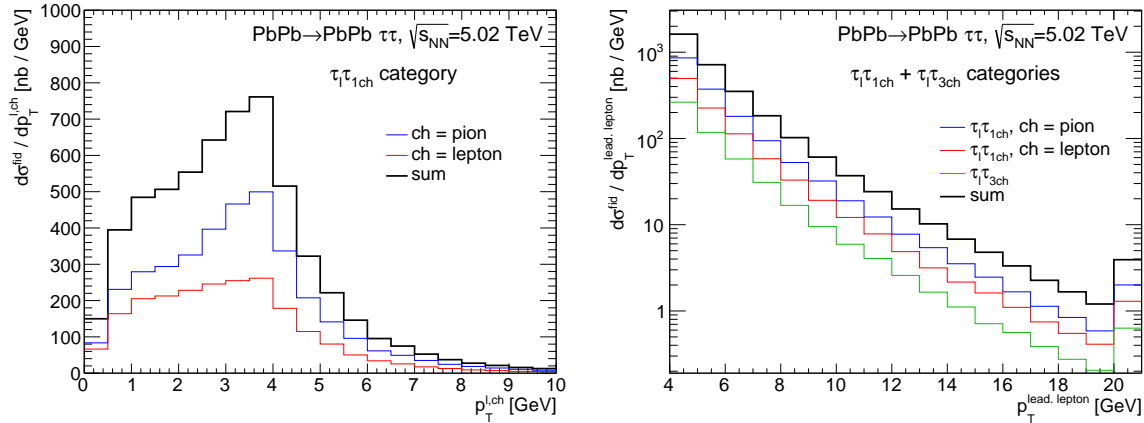


FIG. 5: (Left) Fiducial cross section as a function of p_T of the lepton+track system ($p_T^{\ell ch}$) in the $\tau_\ell\tau_{1ch}$ category for SM scenario ($a_\tau = 0$) and before applying $p_T^{\ell ch} > 1$ GeV requirement. (Right) Fiducial cross section as a function of p_T of the leading lepton for various event categories and the SM scenario ($a_\tau = 0$). The last bin denotes integrated fiducial cross section above $p_T^{\text{lead, lepton}} = 20$ GeV.

sections. The integrated fiducial cross section values are 2630 nb for $\tau_\ell\tau_{1ch}$ category (including 1650 nb for $\ell^\pm\pi^\mp$ decays, 980 nb for $\ell^\pm\ell^\mp$ decays) and 515 nb for $\tau_\ell\tau_{3ch}$ category, assuming Pb+Pb collision energy of $\sqrt{s_{NN}} = 5.02$ TeV.

IV. RESULTS AND DISCUSSION

Figure 6 summarizes the fiducial cross section for $\text{Pb+Pb} \rightarrow \text{Pb+Pb} + \tau^+\tau^-$ process as a function of the leading lepton p_T ($p_T^{\text{lead, lepton}}$) for SM scenario ($a_\tau = 0$) as well as other representative values of a_τ ($a_\tau = -0.1, -0.05, -0.02, 0.02, 0.05, 0.1$). In addition to the overall cross section enhancement, induced by non-zero a_τ , there is an interesting change in the shape of $p_T^{\text{lead, lepton}}$ distribution visible. This is due to the fact that the anomalous τ couplings are more sensitive to higher τ energies, based on the term $\sigma^{\mu\nu}q_\nu$ in Eq. (2.3). There is also an asymmetry between the cross sections for positive and negative a_τ values, which is due to interference between the SM part and the anomalous τ coupling (see Fig. 2).

The integrated fiducial cross sections for different a_τ values are summarized in Table I. This table also lists the expected number of reconstructed events in ATLAS or CMS, assuming 80% reconstruction efficiency within the fiducial region and two values of integrated luminosity (L_{int}): $L_{int} = 2 \text{ nb}^{-1}$ (existing LHC Pb+Pb dataset) or $L_{int} = 20 \text{ nb}^{-1}$ (expected High Luminosity LHC, HL-LHC, dataset) at $\sqrt{s_{NN}} = 5.02$ TeV. With the existing Pb+Pb dataset we expect each experiment to reconstruct about 5000 $\gamma\gamma \rightarrow \tau^+\tau^-$ events ($a_\tau = 0$). The expected number of reconstructed τ pairs grows to about 50 000 at the HL-LHC.

Figure 7 shows the ratio (denoted as R_ℓ) of fiducial cross sections presented in Fig. 6 to the fiducial cross sections from the standard candle process $\gamma\gamma \rightarrow \ell^+\ell^-$ ($\ell = e$ or μ). To calculate these cross sections, the same theoretical framework described in Sec. II is used. The QED FSR effect is modeled by PYTHIA8. To match the fiducial selection of

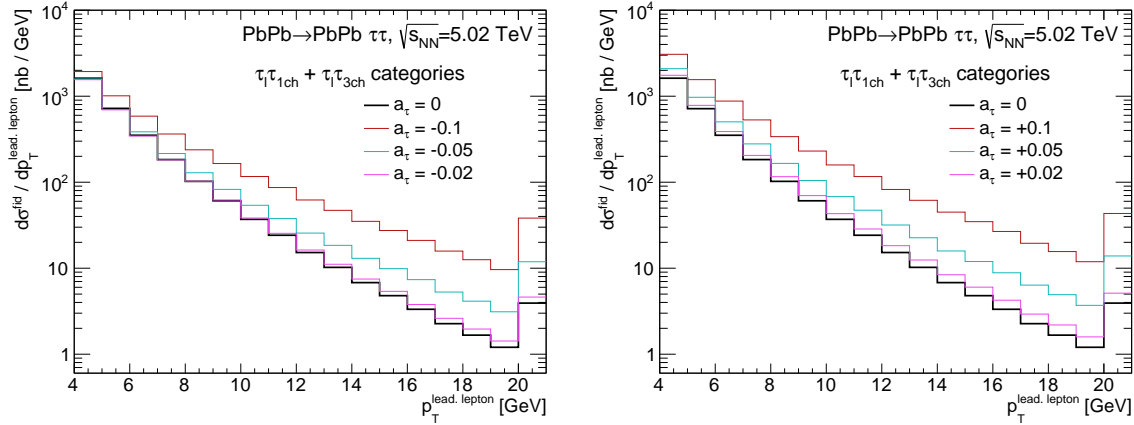


FIG. 6: Fiducial cross section as a function of p_T of the leading lepton for all event categories summed together and various a_τ values: $a_\tau = -0.1, -0.05, -0.02, 0$ (left) and $a_\tau = 0, 0.02, 0.05, 0.1$ (right). The last bin denotes integrated fiducial cross section above $p_T^{\text{lead lepton}} = 20$ GeV.

a_τ value	σ_{fid} [nb]	Expected events	
		($L_{int} = 2 \text{ nb}^{-1}, C = 0.8$)	($L_{int} = 20 \text{ nb}^{-1}, C = 0.8$)
-0.1	4770	7650	76 500
-0.05	3330	5350	53 500
-0.02	3060	4900	49 000
0 (SM)	3145	5050	50 500
+0.02	3445	5500	55 000
+0.05	4350	6950	69 500
+0.1	7225	11550	115 500

TABLE I: Integrated fiducial cross sections for $\text{Pb+Pb} \rightarrow \text{Pb+Pb} + \tau^+ \tau^-$ process for different a_τ values. The expected number of events assuming 80% selection efficiency and $L_{int} = 2 \text{ nb}^{-1}$ (current LHC Pb+Pb dataset) or $L_{int} = 20 \text{ nb}^{-1}$ (expected HL-LHC dataset) are also shown.

$\gamma\gamma \rightarrow \tau^+ \tau^-$ signal process, each lepton is required to have $p_T > 4$ GeV and $|\eta| < 2.5$. The advantage of studying the cross section ratios is the cancellation of several systematic uncertainties, such as the error on integrated luminosity, uncertainties related to lepton reconstruction, but also theoretical uncertainties, e.g. those that are associated with modeling of the initial photon fluxes.

The fiducial cross sections for $\gamma\gamma \rightarrow e^+ e^-$ and $\gamma\gamma \rightarrow \mu^+ \mu^-$ processes are found to be identical, hence one can equally use either of the process. Experimentally, one can match $\tau_e \tau_{1(3)ch}$ channels with $e^+ e^-$ events and $\tau_\mu \tau_{1(3)ch}$ channels with $\mu^+ \mu^-$ events to maximize cancellation of systematic uncertainties.

The sensitivity of the a_τ measurement on modeling of initial photon fluxes can be tested by repeating the analysis using the photon-photon luminosity prediction from the STARLIGHT [41] program. As already demonstrated in Sec. II, the differences in the cross sections between STARLIGHT and the results presented in this work can be as large as 20%, mainly due to extra requirements applied in the modelling of single photon flux in

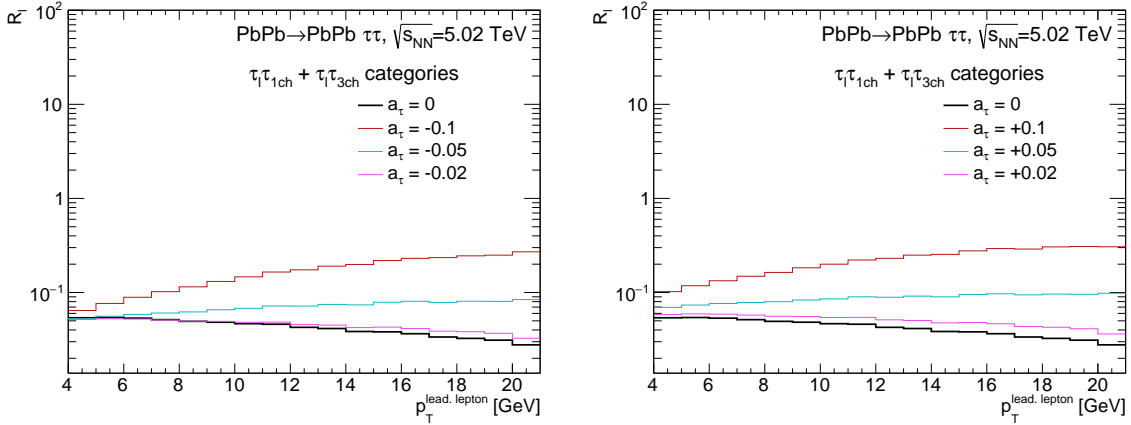


FIG. 7: Ratio of the fiducial cross sections between $\gamma\gamma \rightarrow \tau^+\tau^-$ and $\gamma\gamma \rightarrow \ell^+\ell^-$ ($\ell = e$ or μ) processes as a function of p_T of the leading lepton for all event categories summed together and different a_τ values: $a_\tau = -0.1, -0.05, -0.02, 0$ (left) and $a_\tau = 0, 0.02, 0.05, 0.1$ (right). The last bin denotes the ratio of integrated fiducial cross sections above $p_T^{\text{lead lepton}} = 20$ GeV.

STARLIGHT.

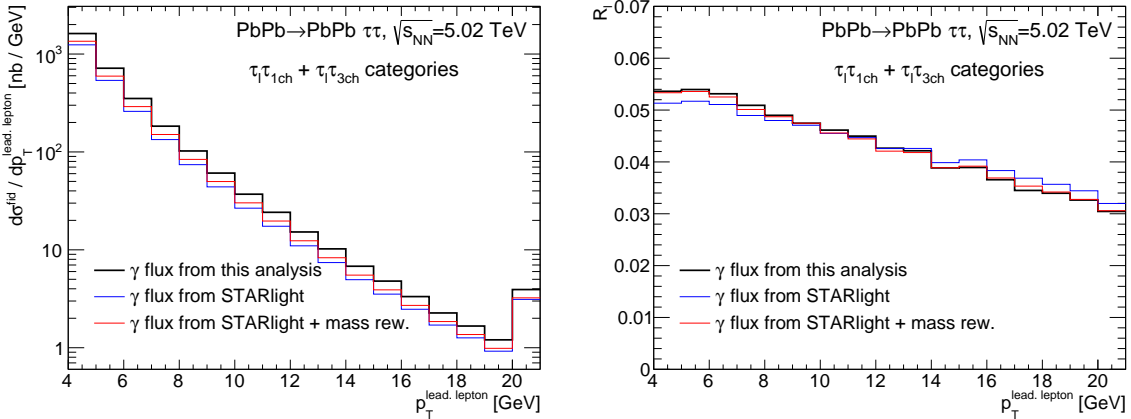


FIG. 8: Fiducial cross section for the $\gamma\gamma \rightarrow \tau^+\tau^-$ process (left) and the ratio of fiducial cross sections between $\gamma\gamma \rightarrow \tau^+\tau^-$ and $\gamma\gamma \rightarrow \ell^+\ell^-$ ($\ell = e$ or μ) processes (right) as a function of p_T of the leading lepton for all event categories summed together and various photon fluxes. The red curve shows the results with extra $m_{\ell\ell}$ shape reweighting as described in the text. The last bin denotes integrated fiducial cross section (or the ratio) above $p_T^{\text{lead lepton}} = 20$ GeV.

Figure 8 shows the fiducial cross section for $\gamma\gamma \rightarrow \tau^+\tau^-$ process in Pb+Pb UPC at the LHC and its ratio (R_ℓ) to the fiducial cross section from $\gamma\gamma \rightarrow \ell^+\ell^-$ ($\ell = e$ or μ) process for the two choices of initial photon fluxes. As expected, the difference in the absolute value of the fiducial cross sections is about 20%. However, after taking the ratio to $\gamma\gamma \rightarrow \ell^+\ell^-$ process, the difference becomes suppressed to 5%. The remaining difference can be explained by the $m_{\ell\ell}$ shape difference between two implementations (as demonstrated already in Figure 3) and the fact that the p_T of the lepton from τ decay does not necessarily correspond to the p_T of lepton from $\gamma\gamma \rightarrow \ell^+\ell^-$ process. It is also demon-

strated in Figure 8 that an extra reweighting of the shape of $m_{\ell\ell}$ distribution would lead to differences in the ratio that are less than 1%. However, it should be noted that in reality the $m_{\ell\ell}$ spectrum can be reweighted directly to the experimental data, thus reducing significantly the impact of theory modelling uncertainties on the measurement.

The expected number of events from Table I can be translated into expected sensitivity for probing a_τ . We use the ROOFIT toolkit [48] for the statistical analysis of the results. We perform fits to $R_\ell(p_T^{lead\ lepton})$ distribution by treating SM results ($a_\tau = 0$) as background and the difference between $a_\tau = 0$ and $a_\tau = X$ distributions as signal. A test statistic based on the profile likelihood ratio [49] is used under the Asimov approximation. The procedure exploits both normalization and $p_T^{lead\ lepton}$ shape differences, providing extra sensitivity on a_τ measurement. We use two values of expected systematic uncertainty (5% and 1%) and two assumptions on Pb+Pb integrated luminosity (2 nb^{-1} to reflect existing ATLAS/CMS dataset, or 20 nb^{-1} for HL-LHC expectations).

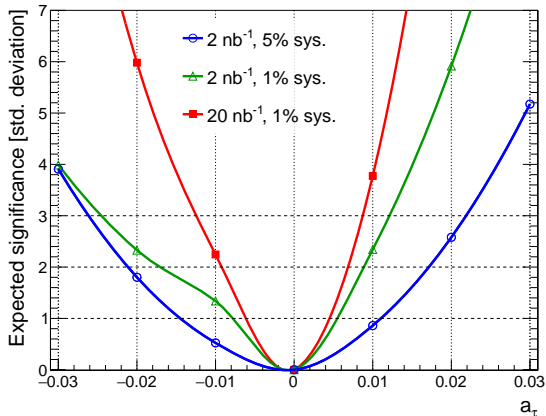


FIG. 9: Expected signal significance as a function of a_τ for various assumptions on Pb+Pb integrated luminosity (2 nb^{-1} or 20 nb^{-1}) and total systematic uncertainty (5% or 1%).

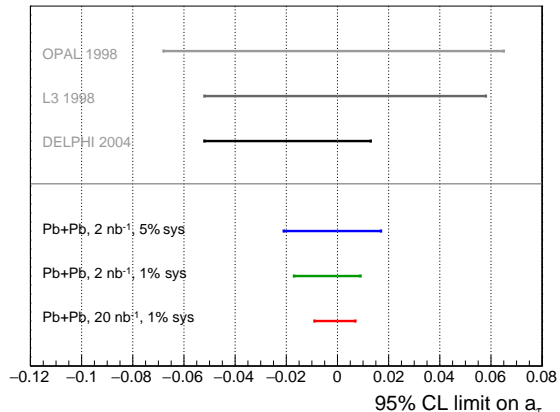


FIG. 10: Expected 95% CL limits on a_τ measurement for various assumptions on Pb+Pb integrated luminosity (2 nb^{-1} or 20 nb^{-1}) and total systematic uncertainty (5% or 1%). Comparison is also made to the existing limits from OPAL [13], L3 [12] and DELPHI [11] experiments at LEP.

Figure 9 shows expected signal significance as a function of a_τ . The observed asymmetry in sensitivity between positive and negative a_τ values reflects the destructive interference between SM and the anomalous τ coupling.

The expected significance can be directly transformed into expected 95% CL limits on a_τ , shown in Fig. 10. Assuming 2 nb^{-1} of integrated Pb+Pb luminosity and 5% systematic uncertainty, the expected limits are $-0.021 < a_\tau < 0.017$, approximately two times better than DELPHI limits [11]. By collecting more data (20 nb^{-1}) and with improved systematic uncertainties, these limits can be further improved by another factor of two. The expected results by studying ultraperipheral collisions at the LHC have therefore the potential to significantly improve the existing limits on a_τ .

In addition, using the same methods we study the sensitivity on tau lepton electric dipole moment, d_τ . Our expected 95% CL sensitivity on $|d_\tau|$ assuming $a_\tau = 0$

is: $|d_\tau| < 6.3 (4.4) \cdot 10^{-17} e \cdot \text{cm}$ at the LHC with 5% (1%) systematic uncertainty and $|d_\tau| < 3.5 \cdot 10^{-17} e \cdot \text{cm}$ at HL-LHC (1% systematic uncertainty). For comparison, the current best limits are measured by Belle experiment [21]: $-2.2 < \text{Re}(d_\tau) < 4.5 (10^{-17} e \cdot \text{cm})$ and $-2.5 < \text{Im}(d_\tau) < 0.8 (10^{-17} e \cdot \text{cm})$. Our projected results on d_τ can be therefore competitive with Belle limits.

The expected limits on a_τ and d_τ are found to be approximately factor of two weaker than those reported in Ref. [35]. This likely points to the issue with EFT approach and the conversion used between the relevant EFT operators and a_τ when calculating elementary $\gamma\gamma \rightarrow \tau^+\tau^-$ cross section.

V. CONCLUSIONS

In this paper, we derived a prediction on the differential cross section of the $\gamma\gamma \rightarrow \tau^+\tau^-$ process and its dependence on anomalous electromagnetic couplings of the tau lepton in ultraperipheral Pb+Pb collisions at the LHC. In contrast to previous calculations, which are based on an effective field theory approach, our calculation is derived from first principles and yields a significantly different inclusive cross section dependence on a_τ than previously reported [35]. We also investigated the expected sensitivity on a_τ and d_τ , assuming standard LHC detectors using the currently available as well as future datasets. In particular we propose to use cross section ratios of the $\gamma\gamma \rightarrow \tau^+\tau^-$ and $\gamma\gamma \rightarrow e^+e^- (\mu^+\mu^-)$ processes to probe a_τ , as several systematic uncertainties cancel and the experimental knowledge of a_e and a_μ is several orders of magnitude more precise than a_τ itself. Our studies suggest that the currently available datasets of the LHC experiments are already sufficient to improve the sensitivity on a_τ by a factor of two, hence, we consider this analysis as highly interesting and worthwhile to be done in the future. Future Belle-II experiment should give much better constraints on $|a_\tau| < 1.75 \cdot 10^{-5}$ and $|d_\tau| < 2.04 \cdot 10^{-19} e \cdot \text{cm}$ [26].

Acknowledgements

We are indebted to Otto Nachtmann for a fruitful discussion. This study was partially supported by the Polish National Science Center grant UMO-2018/31/B/ST2/03537 and by the Center for Innovation and Transfer of Natural Sciences and Engineering Knowledge in Rzeszów.

-
- [1] Gerhard Baur, Kai Hencken, Dirk Trautmann, Serguei Sadovsky, and Yuri Kharlov. Coherent gamma gamma and gamma-A interactions in very peripheral collisions at relativistic ion colliders. *Phys. Rept.*, 364:359–450, 2002. arXiv:hep-ph/0112211, doi:10.1016/S0370-1573(01)00101-6.
 - [2] A. J. Baltz. The Physics of Ultraperipheral Collisions at the LHC. *Phys. Rept.*, 458:1–171, 2008. arXiv:0706.3356, doi:10.1016/j.physrep.2007.12.001.

- [3] STAR Collaboration. Production of e^+e^- pairs accompanied by nuclear dissociation in ultra-peripheral heavy ion collision. *Phys. Rev.*, C70:031902, 2004. arXiv:nucl-ex/0404012, doi: 10.1103/PhysRevC.70.031902.
- [4] PHENIX Collaboration. Photoproduction of J/ψ and of high mass e^+e^- in ultra-peripheral Au+Au collisions at $\sqrt{s} = 200$ GeV. *Phys. Lett.*, B679:321–329, 2009. arXiv:0903.2041, doi:10.1016/j.physletb.2009.07.061.
- [5] ALICE Collaboration. Charmonium and e^+e^- pair photoproduction at mid-rapidity in ultra-peripheral Pb-Pb collisions at $\sqrt{s_{NN}}=2.76$ TeV. *Eur. Phys. J.*, C73(11):2617, 2013. arXiv:1305.1467, doi:10.1140/epjc/s10052-013-2617-1.
- [6] STAR Collaboration. Probing Extreme Electromagnetic Fields with the Breit-Wheeler Process. 2019. arXiv:1910.12400.
- [7] ATLAS Collaboration. Measurement of high-mass dimuon pairs from ultraperipheral lead-lead collisions at $\sqrt{s_{NN}} = 5.02$ TeV with the ATLAS detector at the LHC. Technical Report ATLAS-CONF-2016-025, 2016. URL: <https://cds.cern.ch/record/2157689>.
- [8] ATLAS Collaboration. Evidence for light-by-light scattering in heavy-ion collisions with the ATLAS detector at the LHC. *Nature Phys.*, 13(9):852–858, 2017. arXiv:1702.01625, doi: 10.1038/nphys4208.
- [9] CMS Collaboration. Evidence for light-by-light scattering and searches for axion-like particles in ultraperipheral PbPb collisions at $\sqrt{s_{NN}} = 5.02$ TeV. *Phys. Lett.*, B797:134826, 2019. arXiv:1810.04602, doi:10.1016/j.physletb.2019.134826.
- [10] ATLAS Collaboration. Observation of light-by-light scattering in ultraperipheral Pb+Pb collisions with the ATLAS detector. *Phys. Rev. Lett.*, 123(5):052001, 2019. arXiv:1904.03536, doi:10.1103/PhysRevLett.123.052001.
- [11] DELPHI Collaboration. Study of tau-pair production in photon-photon collisions at LEP and limits on the anomalous electromagnetic moments of the tau lepton. *Eur. Phys. J.*, C35:159–170, 2004. arXiv:hep-ex/0406010, doi:10.1140/epjc/s2004-01852-y.
- [12] L3 Collaboration. Measurement of the anomalous magnetic and electric dipole moments of the tau lepton. *Phys. Lett.*, B434:169–179, 1998. doi:10.1016/S0370-2693(98)00736-9.
- [13] OPAL Collaboration. An Upper limit on the anomalous magnetic moment of the tau lepton. *Phys. Lett.*, B431:188–198, 1998. arXiv:hep-ex/9803020, doi:10.1016/S0370-2693(98)00520-6.
- [14] M. Passera. Precise mass-dependent QED contributions to leptonic $g-2$ at order α^2 and α^3 . *Phys. Rev.*, D75:013002, 2007. arXiv:hep-ph/0606174, doi:10.1103/PhysRevD.75.013002.
- [15] S. Eidelman and M. Passera. Theory of the tau lepton anomalous magnetic moment. *Mod. Phys. Lett.*, A22:159–179, 2007. arXiv:hep-ph/0701260, doi:10.1142/S0217732307022694.
- [16] Dennis J. Silverman and Gordon L. Shaw. Limits on the Composite Structure of the Tau Lepton and Quarks From Anomalous Magnetic Moment Measurements in e^+e^- Annihilation. *Phys. Rev.*, D27:1196, 1983. doi:10.1103/PhysRevD.27.1196.
- [17] Stephen P. Martin and James D. Wells. Muon Anomalous Magnetic Dipole Moment in Supersymmetric Theories. *Phys. Rev.*, D64:035003, 2001. arXiv:hep-ph/0103067, doi: 10.1103/PhysRevD.64.035003.
- [18] A. Gutierrez-Rodriguez, M. A. Hernandez-Ruiz, and L. N. Luis-Noriega. Limits on the dipole moments of the tau lepton via the process $e^+e^- \rightarrow \tau^+\tau^-\gamma$ in a left right symmetric model in a left right symmetric model. *Mod. Phys. Lett.*, A19:2227, 2004. arXiv: hep-ph/0403237, doi:10.1142/S0217732304014689.
- [19] A. Moyotl and G. Tavares-Velasco. Weak properties of the tau lepton via a spin-0 unparticle.

- Phys. Rev.*, D86:013014, 2012. arXiv:1210.1994, doi:10.1103/PhysRevD.86.013014.
- [20] F. Hoogeveen. The Standard Model Prediction for the Electric Dipole Moment of the Electron. *Nucl. Phys.*, B341:322–340, 1990. doi:10.1016/0550-3213(90)90182-D.
- [21] Belle Collaboration. Search for the electric dipole moment of the tau lepton. *Phys. Lett.*, B551:16–26, 2003. arXiv:hep-ex/0210066, doi:10.1016/S0370-2693(02)02984-2.
- [22] W. Bernreuther and O. Nachtmann. CP Violating Correlations in Electron Positron Annihilation Into τ Leptons. *Phys. Rev. Lett.*, 63:2787, 1989. [Erratum: *Phys. Rev. Lett.*64,1072(1990)]. doi:10.1103/PhysRevLett.64.1072.2, 10.1103/PhysRevLett.63.2787.
- [23] W. Bernreuther, O. Nachtmann, and P. Overmann. The CP violating electric and weak dipole moments of the tau lepton from threshold to 500-GeV. *Phys. Rev.*, D48:78–88, 1993. doi:10.1103/PhysRevD.48.78.
- [24] Matteo Fael, Lorenzo Mercolli, and Massimo Passera. Towards a determination of the tau lepton dipole moments. *Nucl. Phys. Proc. Suppl.*, 253-255:103–106, 2014. arXiv:1301.5302, doi:10.1016/j.nuclphysbps.2014.09.025.
- [25] S. Eidelman, D. Epifanov, M. Fael, L. Mercolli, and M. Passera. τ dipole moments via radiative leptonic τ decays. *JHEP*, 03:140, 2016. arXiv:1601.07987, doi:10.1007/JHEP03(2016)140.
- [26] Xin Chen and Yongcheng Wu. Search for the Electric Dipole Moment and anomalous magnetic moment of the tau lepton at tau factories. *JHEP*, 10:089, 2019. arXiv:1803.00501, doi:10.1007/JHEP10(2019)089.
- [27] M. Koksál, A. A. Billur, A. Gutierrez-Rodriguez, and M. A. Hernandez-Ruiz. Model-independent sensitivity estimates for the electromagnetic dipole moments of the τ -lepton at the CLIC. *Phys. Rev.*, D98(1):015017, 2018. arXiv:1804.02373, doi:10.1103/PhysRevD.98.015017.
- [28] A. Gutierrez-Rodriguez, M. Koksál, A. A. Billur, and M. A. Hernandez-Ruiz. Feasibility at the LHC, FCC-he and CLIC for sensitivity estimates on anomalous τ -lepton couplings. 2019. arXiv:1903.04135.
- [29] M. Koksál. Search for the electromagnetic moments of the τ lepton in photon-photon collisions at the LHeC and the FCC-he. *J. Phys.*, G46:065003, 2019. arXiv:1809.01963, doi:10.1088/1361-6471/ab0b53.
- [30] Mark A. Samuel and G. Li. Measuring the magnetic moment of the tau lepton at the Fermilab tevatron, the SSC and the LHC. *Int. J. Theor. Phys.*, 33:1471–1478, 1994. doi:10.1007/BF00670690.
- [31] S. Atag and A. A. Billur. Possibility of Determining τ Lepton Electromagnetic Moments in $\gamma\gamma \rightarrow \tau^+\tau^-$ Process at the CERN-LHC. *JHEP*, 11:060, 2010. arXiv:1005.2841, doi:10.1007/JHEP11(2010)060.
- [32] Alper Hayreter and German Valencia. Constraining τ -lepton dipole moments and gluon couplings at the LHC. *Phys. Rev.*, D88(1):013015, 2013. [Erratum: *Phys. Rev.D*91,no.9,099902(2015)]. arXiv:1305.6833, doi:10.1103/PhysRevD.88.013015, 10.1103/PhysRevD.91.099902.
- [33] Iftah Galon, Arvind Rajaraman, and Tim M. P. Tait. $H \rightarrow \tau^+\tau^-\gamma$ as a probe of the τ magnetic dipole moment. *JHEP*, 12:111, 2016. arXiv:1610.01601, doi:10.1007/JHEP12(2016)111.
- [34] J. Fu, M. A. Giorgi, L. Henry, D. Marangotto, F. Martinez Vidal, A. Merli, N. Neri, and J. Ruiz Vidal. Novel Method for the Direct Measurement of the tau Lepton Dipole Moments. *Phys. Rev. Lett.*, 123(1):011801, 2019. arXiv:1901.04003, doi:10.1103/PhysRevLett.123.011801.

- [35] Lydia Beresford and Jesse Liu. New physics and tau $g - 2$ using LHC heavy ion collisions. 2019. arXiv:1908.05180.
- [36] ATLAS Collaboration. The ATLAS Experiment at the CERN Large Hadron Collider. *JINST*, 3:S08003, 2008. doi:10.1088/1748-0221/3/08/S08003.
- [37] CMS Collaboration. The CMS Experiment at the CERN LHC. *JINST*, 3:S08004, 2008. doi:10.1088/1748-0221/3/08/S08004.
- [38] M. Kłusek-Gawenda and A. Szczurek. Exclusive muon-pair productions in ultrarelativistic heavy-ion collisions – realistic nucleus charge form factor and differential distributions. *Phys. Rev.*, C82:014904, 2010. arXiv:1004.5521, doi:10.1103/PhysRevC.82.014904.
- [39] Andreas van Hameren, Mariola Kłusek-Gawenda, and Antoni Szczurek. Single- and double-scattering production of four muons in ultraperipheral $PbPb$ collisions at the Large Hadron Collider. *Phys. Lett.*, B776:84–90, 2018. arXiv:1708.07742, doi:10.1016/j.physletb.2017.11.029.
- [40] Mariola Kłusek-Gawenda, Piotr Lebiedowicz, Otto Nachtmann, and Antoni Szczurek. From the $\gamma\gamma \rightarrow p\bar{p}$ reaction to the production of $p\bar{p}$ pairs in ultraperipheral ultrarelativistic heavy-ion collisions at the LHC. *Phys. Rev.*, D96(9):094029, 2017. arXiv:1708.09836, doi:10.1103/PhysRevD.96.094029.
- [41] Spencer R. Klein, Joakim Nystrand, Janet Seger, Yuri Gorbunov, and Joey Butterworth. STARlight: A Monte Carlo simulation program for ultra-peripheral collisions of relativistic ions. *Comput. Phys. Commun.*, 212:258–268, 2017. arXiv:1607.03838, doi:10.1016/j.cpc.2016.10.016.
- [42] Torbjörn Sjöstrand, Stefan Ask, Jesper R. Christiansen, Richard Corke, Nishita Desai, Philip Ilten, Stephen Mrenna, Stefan Prestel, Christine O. Rasmussen, and Peter Z. Skands. An Introduction to PYTHIA 8.2. *Comput. Phys. Commun.*, 191:159–177, 2015. arXiv:1410.3012, doi:10.1016/j.cpc.2015.01.024.
- [43] Philip Ilten. Tau Decays in Pythia 8. *Nucl. Phys. Proc. Suppl.*, 253-255:77–80, 2014. arXiv:1211.6730, doi:10.1016/j.nuclphysbps.2014.09.019.
- [44] ATLAS Collaboration. Reconstruction of hadronic decay products of tau leptons with the ATLAS experiment. *Eur. Phys. J.*, C76(5):295, 2016. arXiv:1512.05955, doi:10.1140/epjc/s10052-016-4110-0.
- [45] CMS Collaboration. Performance of reconstruction and identification of τ leptons decaying to hadrons and ν_τ in pp collisions at $\sqrt{s} = 13$ TeV. *JINST*, 13(10):P10005, 2018. arXiv:1809.02816, doi:10.1088/1748-0221/13/10/P10005.
- [46] ATLAS Collaboration. Zero degree calorimeters for ATLAS. Technical Report CERN-LHCC-2007-01, 2007. URL: <https://cds.cern.ch/record/1009649>.
- [47] Anthony J. Baltz, Yuri Gorbunov, Spencer R. Klein, and Joakim Nystrand. Two-Photon Interactions with Nuclear Breakup in Relativistic Heavy Ion Collisions. *Phys. Rev.*, C80:044902, 2009. arXiv:0907.1214, doi:10.1103/PhysRevC.80.044902.
- [48] Wouter Verkerke and David P. Kirkby. The RooFit toolkit for data modeling. *eConf*, C0303241:MOLT007, 2003. arXiv:physics/0306116.
- [49] Glen Cowan, Kyle Cranmer, Eilam Gross, and Ofer Vitells. Asymptotic formulae for likelihood-based tests of new physics. *Eur. Phys. J.*, C71:1554, 2011. [Erratum: *Eur. Phys. J.*C73,2501(2013)]. arXiv:1007.1727, doi:10.1140/epjc/s10052-011-1554-0, 10.1140/epjc/s10052-013-2501-z.